Acta Cryst. (1995). D**51**, 541–549

Molecular Dynamics and Structure-Based Drug Design for Predicting Non-natural Nonapeptide Binding to a Class I MHC Protein

BY LEONARDO SCAPOZZA,† DIDIER ROGNAN‡ AND GERD FOLKERS

Swiss Federal Institute of Technology, Department of Pharmacy, CH-8057 Zürich, Switzerland

AND ANGELIKA DASER

Deutsches Rheumaforschungszentrum, D-13353 Berlin, Germany

(*Received* 2 *June* 1994; *accepted* 22 *February* 1995)

Abstract

Starting from the known three-dimensional structure of the class I major histocompatibility complex-encoded HLA-B*2705 protein, three non-natural nonapeptides were designed to fit optimally the HLA-B*2705-binding groove. The optimization was performed using structure-based drug design methods and the fact that all the possible interactions of the secondary anchor residue (position 3) with its human leukocyte antigen-binding pocket (pocket *D*) in nature are not entirely utilized. 150 ps molecular-dynamics (MD) simulation in water was employed to study the stability of the bimolecular complexes with three non-natural peptides (*P*3 = homophenylalanine, β-naphthylalanine, α-naphthylalanine) as well as with the two natural homologues (*P*3 = Gly, Leu). Various structural and dynamical properties (atomic fluctuations, solvent-accessible surface areas, peptide Cα-atom positions) of the simulated bimolecular complexes were used to compare the three non-natural with the two natural ligands. Since the various molecular properties have been shown previously to be related to the binding affinity of nonapeptide ligands to the major histocompatibility complex (MHC) HLA-B*2705 protein, the MD data predict a rather higher stability of MHC–ligand complexes with the three non-natural peptides, suggesting that the unnatural peptides studied show an enhanced binding affinity to the HLA-B*2705 protein. These results are in agreement with the experimental values of a semi-quantitative *in vitro* assembly assay, performed on the five nonapeptides (*P*3 = Gly, Leu, homophenylalanine, β-naphthylalanine, α-naphthylalanine), which shows their ability to stabilize the native conformation of the HLA-B*2705 heavy chain and also shows that the three non-natural ligands bind with higher affinity (0.5 μ*M*) to the MHC protein than the two natural homologues (40 μ*M*). Thus, this study demonstrates that structural information combined with rational design and molecular-dynamics simulations can illustrate and predict MHC binding and potential T-cell epitope properties as well as contribute to the design of new non-peptidic MHC inhibitors that may be useful for the selective immunotherapy of autoimmune diseases to which HLA alleles are directly associated.

Abbreviations

MHC, major histocompatibility complex; HLA: human leukocyte antigen; TCR, T-cell receptor; CTL, cytotoxic T-lymphocytes; MD, molecular dynamics; r.m.s., root-mean square; Hpa, homophenylalanine; Ana, α-naphthylalanine; Bna, β-naphthylalanine; SDS–PAGE, sodium dodecyl sulfate polyacrylamide gel electrophoresis.

Introduction

Class I MHC molecules are polymorphic glycoproteins whose function is to recognize and load intracellular antigenic peptides as well as present them at the surface of infected cells to cytotoxic T lymphocytes (Townsend & Bodmer, 1989; Bjorkman & Parham, 1990). Since the description of the first class I MHC protein (HLA-A2.1) by X-ray diffraction (Bjorkman *et al.*, 1987), more crystal structures of MHC–peptide complexes have been described to date for class I MHC: HLA-A2.1 (Madden, Garboczi & Wiley, 1993), HLA-Aw68 (Silver, Guo, Strominger & Wiley, 1992), HLA-B27 (Madden, Gorga, Strominger & Wiley, 1991, 1992) and H-2k^b molecules (Fremont, Matsamura, Stura, Peterson & Wilson, 1992; Zhang, Young, Imarai, Nathenson & Sachettini, 1992). Based on the crystallographic and immunological information several attempts have been made to understand the molecular basis of the cellular immune response (see, Madden & Wiley, 1992). In all cases, the bound peptide (preferentially a nonamer) presents a rather extended conformation with conserved electrostatic interactions (salt bridges, hydrogen bonds) between its backbone atoms and invariant MHC side chains, and allele-specific interactions between specific

† Current address: Texas A & M University, Department of Biochemistry and Biophysics, 77843-2128 College Station, Texas, USA.

‡ Author to whom correspondence should be addressed.

side chains [often at positions 2 and 9 (*P*2 and *P*9)] and polymorphic MHC pockets (Fig. 1). The amino acids of the nonamer can be ordered into three functional regions. The first one contains the major anchor residues that are located at positions 2 (*P*2) and 9 (*P*9). *P*2 is highly conserved within the peptide repertoire while *P*9 is more variable (Falk, Rötzschke, Stevanovic, Jung & Rammensee, 1991; Rötzscke *et al.*, 1994). The second one contains the secondary anchor residues (positions 1 and 3) which are more variable. The third one, located in the middle of the peptide (*P*4–*P*8), is highly variable, bulges out of the binding groove and probably contacts a T-cell receptor in the MHC–peptide–TCR ternary complex (Fremont *et al.*, 1992). The recognition of a MHC–peptide complex by a TCR may result in either protective physiological responses to viral or bacterial infections or lead to pathological events upon disregulation of the cellular immune system, often resulting from 'alloreaction' (rejection of non-histocompatible tissue transplants, autoimmune diseases) (Zinkernagel & Doherty, 1974). One of the strongest linkages known to date is the association between the serologically defined HLA-B27 family of class I MHC molecules (HLA-B*2701, HLA-B*2702, HLA-B*2704 and HLA-B*2705; 1990 World Health Organization nomenclature) and inflammatory spondyloarthropathies such as ankylosing spondylitis (Brewerton *et al.*, 1973) or reactive arthritis (Kingsley & Sieper, 1993). Blocking selectively the class I MHC-binding groove without triggering any CTL response would then be highly desirable in order to stop the course of these diseases. This therapeutical target may be reached by non-stimulatory MHC ligands (peptidic or not) that could successfully compete with auto antigens (Adorini *et al.*, 1988; Evavold, Sloan-Lancaster & Allen, 1993). In this report, we document the usefulness of structure-based drug design and molecular-dynamic simulations for the illustration and prediction of MHC-binding and T-cell epitope properties. It is not our intention to propose a quantitative hierarchy of binding for the peptides presented, but rather to illustrate the stability of the different MHC–peptide complexes by various molecular properties that have been previously shown to discriminate binding from non-binding peptides (Rognan, Scapozza, Folkers & Daser, 1994).

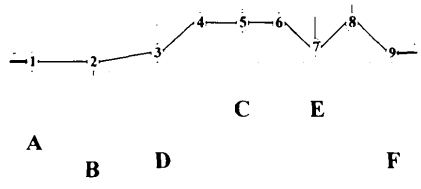

Fig. 1. Schematic representation of nonapeptide binding to class I MHC proteins, exemplified by HLA-B27 (Madden *et al.*, 1992), where the main anchor side chains at *P*2 and *P*9 interact with pockets *B* and *F*, respectively. The secondary anchors at *P*1, *P*3, *P*5 and *P*7 can contact either a TCR or the MHC itself. Positions 4 and 8 are potential TCR-contact residues.

Methods

Program and parameters

Molecular mechanics and dynamics simulations were performed using the *AMBER* 4.0 program (Weiner *et al.*, 1984) and the standard parm91 parameter set (Pearlman *et al.*, 1992). New residue topology files were created for non-standard amino acids (Hpa, Ana, Bna) from semi-empirical *MOPAC* 5.1 PM3 geometries (Stewart, 1990) and potential-derived atomic charges resulting from an *MNDO* (Dewar & Thiel, 1977) single-point SCF calculation as described by Besler, Merz & Kollman (1990). All calculations were run on a Cray Y-MP/264. Graphic display and analysis of molecular-dynamics simulations were achieved with the *SYBYL* molecular-modeling package (Tripos Associates Inc., 1992) and using in-house routines (Krug, 1991), respectively. The MD protocol reported by Rognan *et al.* (1994) was used. Comparative analysis of various structural and dynamical properties (atomic fluctuations, solvent-accessible surface areas, peptide Cα-atom positions) for instantaneous and relaxed time-averaged conformations (between 100 and 150 ps) was performed in order to illustrate and predict binding affinity of the non-natural nonapeptides.

Preparation of the input coordinates

The coordinates of the HLA-B*2705 X-ray structure, solved at 2.1 Å resolution (Madden *et al.*, 1992; PDB entry 1HSA), were used as a template. The MHC-bound peptide (*P*3 = Gly) was built by simply substituting side chains according to the published crystal structure that contained a peptide model (RRIKAITLK), using *SYBYL*. Other studied HLA-B*2705-binding nonapeptides (Table 1) were built by substitution of the Gly side chain in position 3 with the corresponding side chains of Leu, Hpa, Ana and Bna. These were positioned in pocket *D* in agreement with the most favorable interaction site between a probe methyl group and the empty HLA-B*2705 subsite *D* calculated by the *GRID* method (Goodford, 1985) with a grid spacing of 0.5 Å. Neither steric nor electrostatic conflicts were discovered between the positioned ligand side chains and the binding-cleft side chains forming the various subsites. In order to save computational time, only the antigen-binding α1-α2 domains (182 residues) were taken into account in the study. This approximation was previously shown not to alter the accuracy of the MD simulations (Rognan, Zimmermann, Jung & Folkers, 1992) because only limited interactions exist between the α1-α2 part and the other two domains (α3 and β_2m) which are not suspected to contact antigenic peptides in

Table 1. *Names and sequence of the studied HLA-B*2705-binding nonapeptides*

Name	Sequence	Origin	Type
P3 = Gly	KR(Gly)IDKAAK	*C. trachomatis* GroEL 117-125	Natural
P3 = Leu	KR(Leu)IDKAAK	Synthesis	Natural
P3 = Hpa	KR(Hpa)IDKAAK	Synthesis	Non-natural
P3 = Bna	KR(Bna)IDKAAK	Synthesis	Non-natural
P3 = Ana	KR(Ana)IDKAAK	Synthesis	Non-natural

the binding groove. The C-terminal residue of the $\alpha 2$ domain (Thr182) was protected by an *N*-methyl group to avoid unrealistic electrostatic interactions. Six crystal water molecules were explicitly taken into account, as they are located in the peptide-binding cleft and take part in the hydrogen-bond network binding the peptide to the protein in the X-ray structure. None of these waters is in pocket *D*. Polar H atoms were then added. Thus, the bimolecular complex and the six crystalline water molecules were centered in a 7.5 Å thick shell of TIP3P water molecules (Jorgensen, Chandrasekhar, Madura, Impey & Klein, 1983) without periodic boundaries or positional constraints on solvent atoms. Any water atom closer than 1.75 Å to any solute atom was discarded, so that approximately 1500 water molecules were added to each MHC–peptide binary complex.

Molecular mechanics and dynamics protocols

AMBER united atom-force-field parameters were used for the MHC–peptide complex in addition to the TIP3P model for simulation in water. Because explicit water molecules were taken into account, the dielectric constant was set to 1. To avoid splitting dipoles, non-bonded interactions were calculated within a residue-based cut-off of 9.0 Å. The solvent atoms were first relaxed by 1000 steps of steepest descent energy minimization, the solute being held fixed. The solvated complex was then fully minimized by 1000 steps of steepest descent followed by a conjugate-gradient minimization procedure until the r.m.s. gradient of the potential energy was less than 0.25 kcal mol^{-1} $Å^{-1}$. The minimized coordinates were thereafter used as the starting point for a 150 ps MD simulation at constant temperature. Initial velocities were taken from a Maxwellian distribution at 50 K. The system was progressively heated from 50 to 297 K during the first picosecond, the temperature being held at 297 K for the rest of the simulation by coupling the system to a heat bath (Ryckaert, Cicotti & Berendsen, 1977) using a temperature coupling constant of 0.05 ps. All bond lengths were constrained to their equilibrium values using the *SHAKE* algorithm (Berendsen, Postma, van Gunsteren, DiNola & Haak, 1984) with a bond length tolerance of 2.5×10^{-4}. Coordinates, energies and velocities were collected and saved every 50 steps (0.1 ps) for 150 ps. Each 150 ps MD simulation of the system, containing 193 amino acids and *ca* 1500 water molecules, required 22 CPU hours on a Cray Y-MP/264.

Solvent-accessible surface areas

Accessible and buried surface areas were computed on energy-minimized time-averaged MHC–peptide structures, by using the *MS* program (Connolly, 1983) with a 1.4 Å radius probe.

In vitro assembly assay

This was performed according to Daser, Henning & Henklein (1994) and Townsend *et al.* (1990). LCL5.2.4 cells (10^7) were labeled with [^{35}S]methionine and lysed in the presence of 100 μM peptide. After overnight incubation, stable HLA-B*2705 molecules were immunoprecipitated with the monoclonal antibody ME1 (Ellis, Taylor & McMichael, 1982) and analyzed by SDS–12% PAGE. Semi-quantitation of the stabilized HLA-B*2705 heavy-chain bands was obtained by densitometry [Howtek (Hudson, NH) Scanmaster 3; NH; PDI software, Huntington Station, NY].

Results and discussion

The starting point of the design process was the 2.1 Å resolution X-ray crystallographic structure of HLA-B*2705 (Madden *et al.*, 1992) complexed with a model peptide (RRIKAITLK). Initially, attention was placed on the secondary anchor residues (*P*1 and *P*3), as well as on residues at positions 5 and 7 (*P*5 and *P*7) and not on the major anchors (*P*2 and *P*9), because enhancing their binding to their respective MHC pockets (*B*, *F*) appears a very difficult task due to the highly specific interactions that are involved (Guo *et al.*, 1993). In order to increase the binding affinity of the peptide to the MHC–protein, the secondary anchor at positions *P*1 as well as *P*5 and *P*7 were rejected for structure-based design because most of their interactions with the HLA-binding groove are accessible to solvent and likely to be easily disturbed.

Only the amino acid in position 3 (*P*3) represents an immediately attractive target for drug-design purposes. Its side chain is directed toward a deep hydrophobic pocket (pocket *D*) but, in case of the natural amino acids, interacts only with the upper part of the subsite (Tyr99, Tyr159) (Fig. 2). This view is supported by the X-ray diffraction studies on HLA-B*2705 which showed that only the upper part of this subsite is filled by extra electron density. These observations indicate that there is a deeply positioned hydrophobic region at the bottom of this subsite, which is unfilled by smaller side chains and, therefore, especially interesting for drug design.

Because of the hydrophobic characteristic of the subsite *D* we have chosen to explore the cavity with a hydrophobic neutral probe. For rationalizing the binding of an hydrophobic side chain to pocket *D*, we computed the optimum interaction site of a neutral methyl probe in the empty pocket using the *GRID* program (Goodford, 1985) which uses simple non-bonded potential functions

(Lennard–Jones, coulomb, hydrogen bonding) to calculate the interaction enthalpies. The resulting well defined negative-energy contour map (at $-2.75\,\text{kcal mol}^{-1}$) is localized within pocket *D* (Fig. 2). Fig. 2 shows that this energy map goes deep into the pocket so that favorable hydrophobic interactions with the two Ile residues at the bottom of the pocket are possible. After graphical inspection we found that the groove was large enough to accommodate bulky side chains (Hpa, Ana and Bna) without modifying the φ,ψ peptide backbone angles or the MHC side chains.

Using MD simulations of class I MHC–peptide bimolecular complexes (Rognan *et al.*, 1994), we assessed the stability of this static model to predict whether the non-natural nonapeptides would bind better than the natural homologues. Therefore, we employed the MD protocol described above. The sequence of an HLA-B*2705-binding bacterial peptide (*P*3 = Gly) (KRGIDKAAK) from the Hsp57 protein of *Chlamydia trachomatis* (Daser *et al.*, 1994) was taken as the lead peptide and substituted at position *P*3 with hydrophobic side chains of increasing sizes (Leu, Hpa, Bna, Ana) (Table 1) in order to create a series of homologous peptides. The resulting nonapeptides were then modeled in the MHC-binding cleft according to the procedure described above.

The equilibrium state of the MD simulation was monitored by observing the r.m.s. deviations of instantaneous structures from the X-ray structure (Fig. 3*a*). These were found to reach a plateau after 100 ps and to be reasonably low (2.3 ± 0.27 Å for backbone atoms). The residues forming the binding groove (α-helical region) and the antiparallel β-sheet region have somewhat smaller r.m.s. backbone deviations with mean values of 1.9 ± 0.31 and 1.4 ± 0.12 Å, respectively. Deviations of the peptide backbone from its experimental structure are low with mean values of 1.1 ± 0.47 Å (an average of values calculated over the last 500 conformations for each simulated complex). Comparable r.m.s. deviation values have already been reported (Rognan *et al.*, 1992, 1994) for other HLA alleles simulated under analogous conditions. These results suggest that the three-dimensional structure of the binding groove will not be distorted by accommodating bulky hydrophobic side chains (Fig. 3*b*).

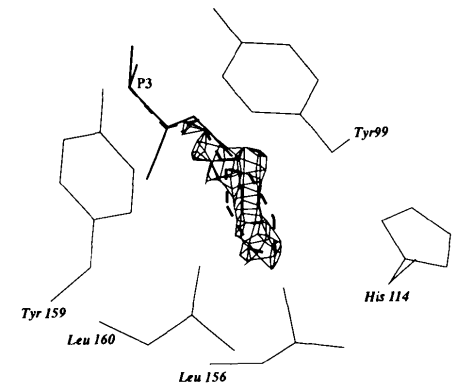

Fig. 2. Grid energy contours map (at -2.75 kcal mol^{-1}) indicating the most favorable interactions between the free HLA-B27 pocket *D* (Tyr99, Hid114, Leu156, Tyr159, Leu160) and a neutral methyl group probe. Leu (solid lines) and Hpa (broken lines) side chains have been fitted to the contour map, in their X-ray and modeled conformations, respectively.

As a second indicator of stability, we computed the buried surface areas of each MHC-bound nonamer in its time-averaged conformation (Fig. 4). Similar patterns are found for the five peptides with major anchors (*P*2, *P*9) extensively buried upon HLA binding, whereas the bulging TCR-interacting domain (*P*4–*P*7) is found to be highly accessible to solvent. Noteworthy is the difference observed at the substituted *P*3 position for which the buried surface area is related to the size of the side chain, confirming our previous *GRID* analysis indicating an unfilled space deep in the pocket. These results predict that the three non-standard nonapeptides should have a higher binding affinity to the MHC-binding site than the natural nonapeptides, the buried surface area being highly correlated to the binding strength (Saito, Peterson & Matsamura, 1993; Rognan *et al.*, 1994). To confirm this hypothesis, r.m.s. atomic fluctuations for all complexes were calculated from time-averaged MD structures (Fig. 5*a*). They show that strong anchors (N terminus, *P*2, *P*9) are found to be much less mobile than the protruding *P*4–*P*8 pentapeptide and that increasing the size of the *P*3 side chain causes a diminution of the r.m.s. fluctuation (the smaller the amino acid at this position, the higher the r.m.s. atomic fluctuations). A complementary picture of the atomic motions of the MHC subsites is displayed in Fig. 5(*b*). Pockets *B* and *F*, which accommodate the side chains of *P*2 and *P*9, respectively, show relative low values in agreement with previous observations (Rognan *et al.* 1994). Pockets *A* and *D*, the secondary anchor residues accommodating subsites (recall Fig. 1), show an interesting pattern which discriminates between natural and non-natural peptides and suggests an enhanced binding affinity for the unnatural peptides.

Moreover a geometrical analysis of time-averaged structures was performed measuring the distance of the Cα atoms of the bound peptide from a binding-site plane. This has been defined from the Cα atoms of all peptide-binding residues located on the α-helical parts of the α1-α2 domain (more details in Fig. 6 caption). The analysis of the positions of the Cα atoms shows clearly the stabilizing effect of the non-natural side chains at *P*3 (Fig. 6). This effect is not only located at *P*3 itself but it is also extended to the major anchor residues *P*2 and *P*9. The effect at *P*3 is reflected in a diminution of the interatomic distance between the backbone N atom of *P*3 (hydrogen-bond donor group) and the acceptor

OH group of Tyr99 (distance calculated for the time-averaged conformation: 6.3 Å for *P*3 = Gly, 4.9 Å for *P*3 = Leu, 3.3 Å for *P*3 = Hpa, 3.5 Å for *P*3 = Ana, 3.3 Å for *P*3 = Bna). This geometrical analysis further suggests an enhanced binding affinity for the three non-natural nonapeptides.

The same predictive indications given by the analysis of the buried surface areas, the r.m.s. fluctuations and the elevation of the Cα atoms of the nonamers from the binding-site plane could be found by analyzing the MHC–peptide hydrogen bonds defined by following criteria: distance between donor *D* and acceptor *A* less than 3.2 Å and *D*—H···*A* angle between 140 and 180°. A total of eight and 13 MHC–peptide hydrogen bonds have been found for *P*3 = Gly and *P*3 = Leu, respectively. When the MHC–peptide interactions are observed for the non-natural peptides, the following number of intermolecular bonds are found: 13 for *P*3 = Bna, 14 for *P*3 = Hpa and 17 for *P*3 = Ana. This shows a conservation as well as an enhancement of the interaction between the nonapeptides backbone and the binding groove for the three non-natural ligands compared to their natural homologues.

These results, and those of previous analyses showing that buried surface areas as well as r.m.s. fluctuations could be related to the binding capacity of the nonapeptides to this HLA protein (Rognan *et al.*, 1994), let us conclude and predict that the three non-natural nonapeptides would present an enhanced binding affinity to the HLA-B*2705 protein.

To probe our model, all five nonamers were synthesized, purified and tested in an *in vitro* assembly assay

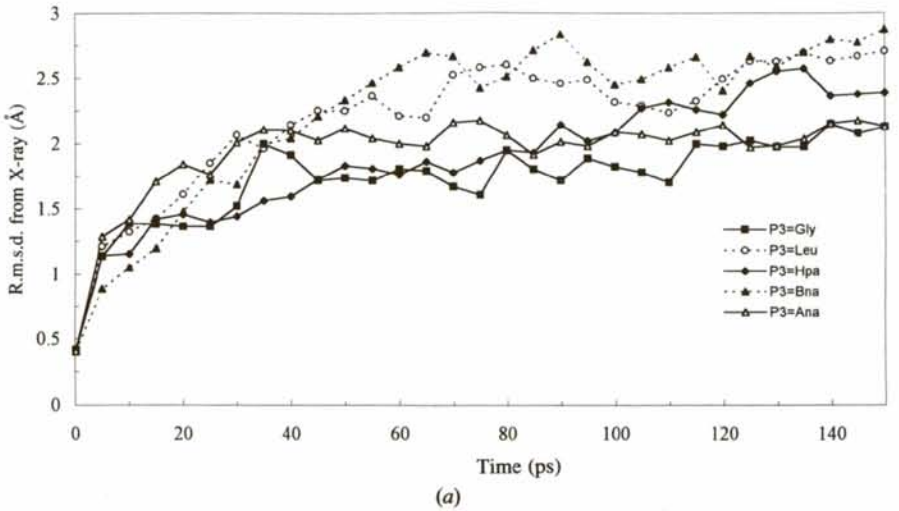

(*a*)

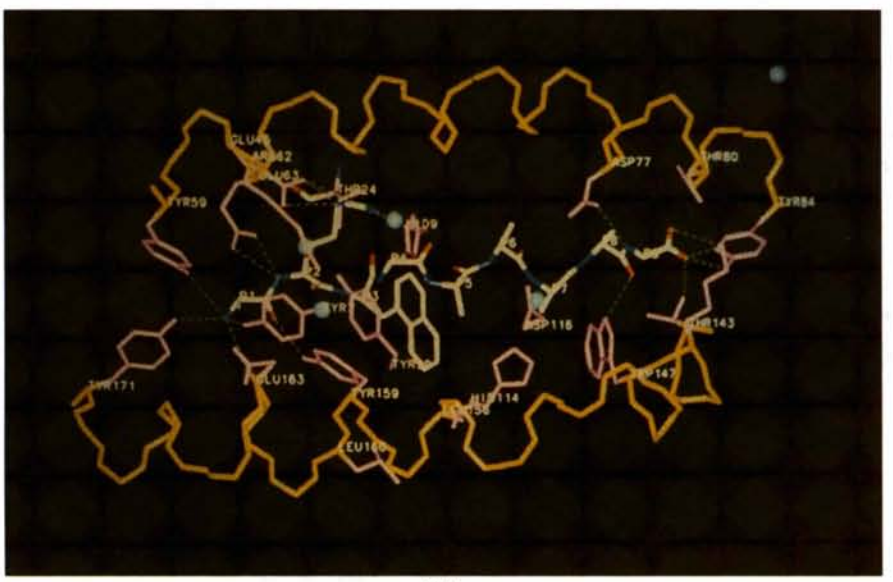

(b)

Fig. 3. (*a*) R.m.s. deviations of HLA-B27 backbone atoms from the crystal structure during the 150 ps MD simulation of HLA-B*2705 in complex with five different nonapeptides (see Table 1). (*b*) Time-averaged conformation of HLA-B27 in complex with one nonapeptide (*P*3 = Ana) as a representative example. The backbone atoms of the two α-helices determining the peptide-binding site are displayed here (in yellow) with the side chains of peptide-binding residues (in magenta). *P*1 (N terminus) to *P*9 (C terminus) are the labels for the Cα positions of bound peptides (in atom-encoded color). Only the peptide-anchor side chains are shown. The six crystal water molecules are represented by spheres (in cyan) and the MHC–peptide hydrogen bonds by green broken lines. Criteria for hydrogen bond: a donor (*D*) to acceptor (*A*) distance less than 3.2 Å and a *D*—H···*A* angle value in the range 140–180°. It shows the typical extended conformation of the bound peptide with conserved electrostatic interactions as well as the maintenance of the three-dimensional structure.

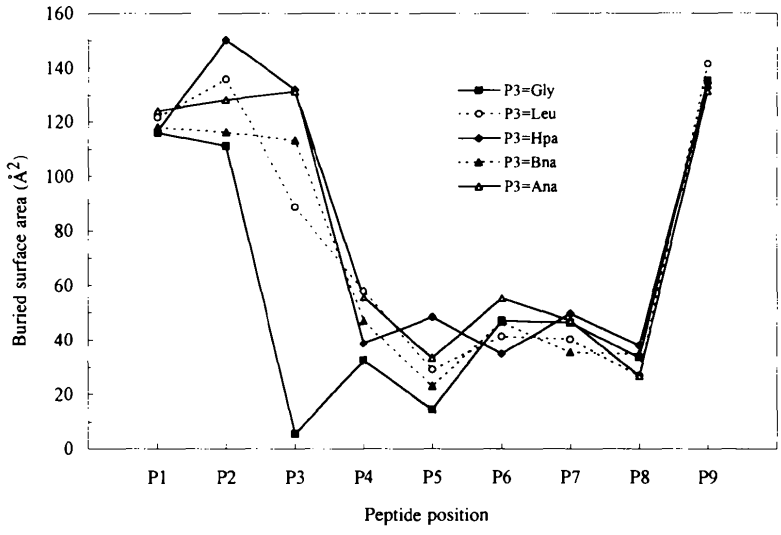

Fig. 4. Buried surface areas of HLA-B27-bound peptides, calculated from relaxed time-averaged conformations (between 100 and 150 ps). Surface areas were calculated using the *MS* program (Connolly, 1983) with a 1.4 Å radius probe. The sequence of the bound peptide (Lys-Arg-Xaa-Ile-Asp-Lys-Ala-Ala-Lys) varies only at position 3. Low values imply that the residue is more exposed to the solvent and less tightly bound to the MHC-binding site.

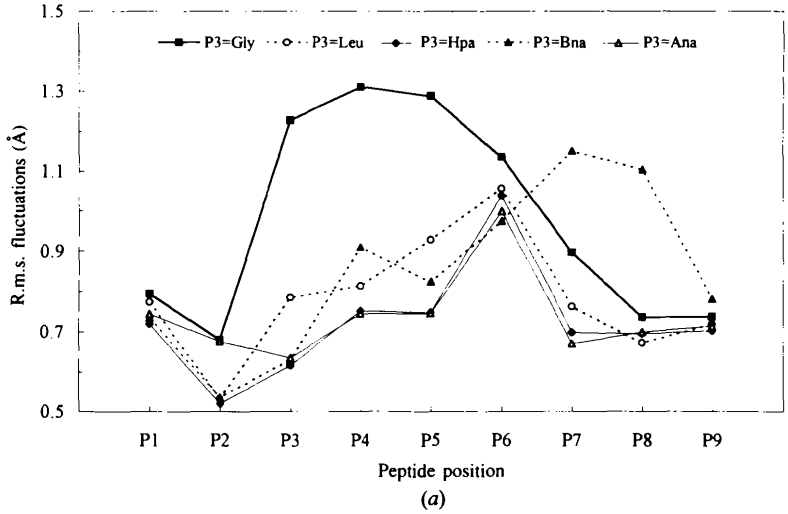

(*a*)

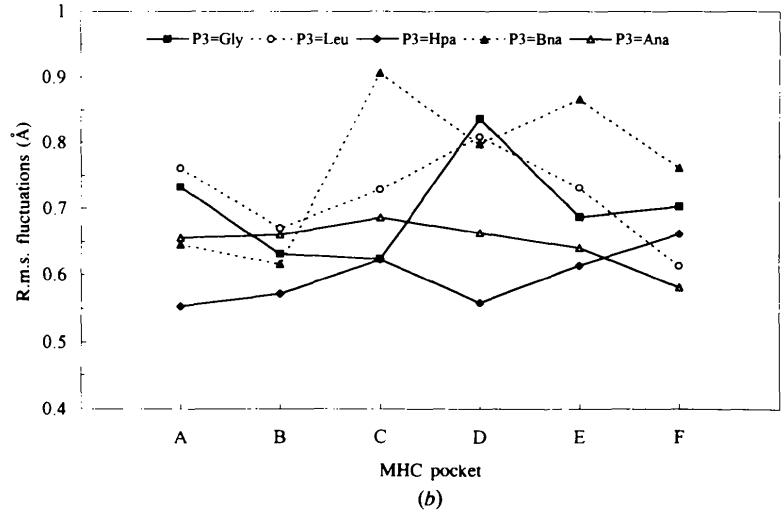

(*b*)

Fig. 5. (*a*) R.m.s. atomic fluctuations of HLA-B*2705-bound peptides (averaged per peptide residue over the backbone atoms) and calculated from time-averaged conformations between 100 and 150 ps. The sequence of the bound peptide (Lys-Arg-Xaa-Ile-Asp-Lys-Ala-Ala-Lys) varies only at position 3. The diminution of the r.m.s. fluctuation reveals an increased stability of the nonamer because of the higher binding affinity to the MHC protein. (*b*) R.m.s. atomic fluctuations of the six HLA-B*2705 specificity pockets (all atoms) for the HLA in complex with the five peptides whose sequence (Lys-Arg-Xaa-Ile-Asp-Lys-Ala-Ala-Lys) varies only at position 3. Fluctuations were calculated from time-averaged conformations between 100 and 150 ps. The pockets were defined according to Saper, Bjorkman & Wiley (1991) and Rognan *et al.* (1994) [pocket *D* (Tyr99, His114, Leu156, Tyr159, Leu160)]. The diminution of the r.m.s. fluctuation reveals an increased interaction between the side chains of the bound peptide and the MHC subsites, which stabilize the bimolecular complex.

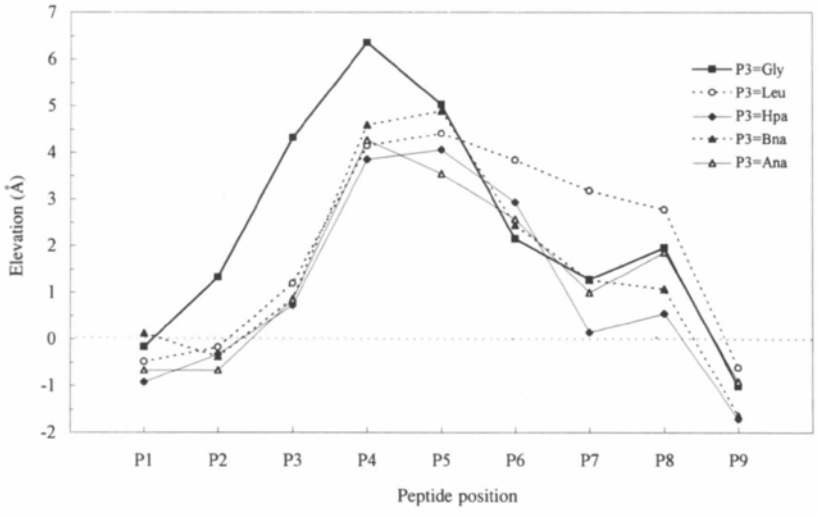

Fig. 6. Elevation of the Cα atoms of the nonapeptides from the binding-site plane calculated for time-averaged conformations. This plane has been defined from the Cα atoms of all peptide-binding residues located on the α-helical parts of the α1-α2 domain (Tyr59, Glu63, Ile66, Lys70, Asp74, Asp77, Thr80, Tyr80, Thr143, Lys146, Trp147, Ala150, Val152, Leu156, Tyr159, Leu160, Glu163, Trp167, Tyr171). Low values indicate a location of the Cα atoms closer to the floor of the binding groove.

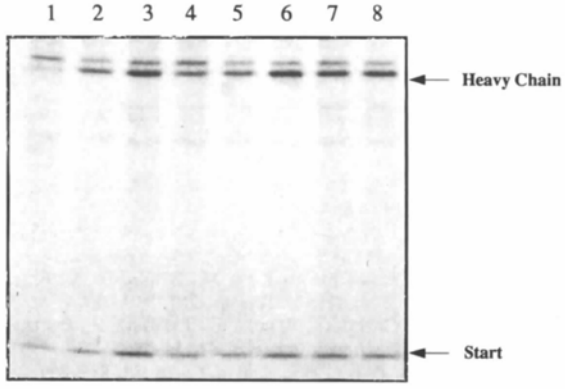

(*a*)

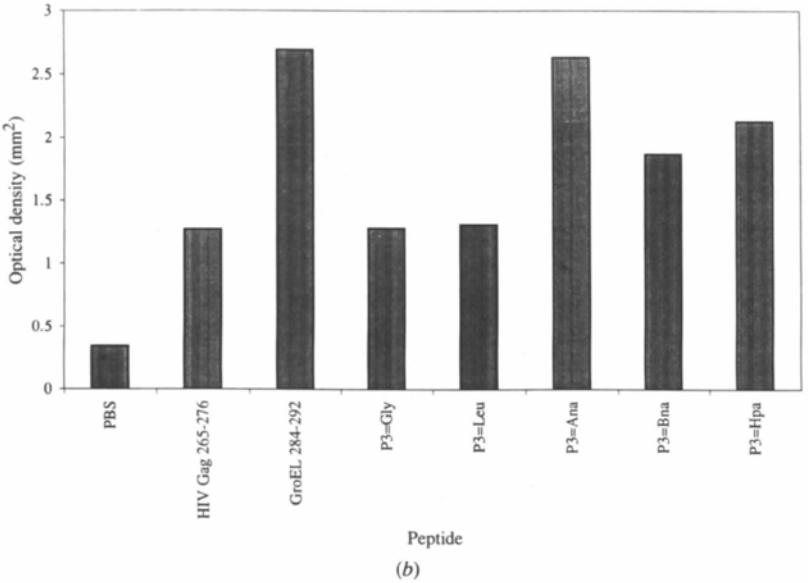

(*b*)

Fig. 7. Effect of *P*3 substitution on the binding of the studied nonapeptides (Table 1) to the HLA-B*2705. (*a*) Autoradiograph of the *in vitro* assembly assay. The lower band is the HLA-B*2705 heavy chain; the upper band is given by non-specific coprecipitation (Daser *et al.*, 1994). Lane 1, phosphate-buffered saline (PBS) control (negative control); lane 2, human immunodeficiency virus (HIV) *Gag* (265–276) (K*R*WIILGLN*K*IV) (Huet *et al.*, 1990) middle–strong binding peptide: binding 40 $\simeq \mu M$; lane 3, *Chlamydia trachomatis GroEL* (284–292) (R*R*KAMFED*I*), strong binding peptide: binding $\simeq 0.5\,\mu M$ (Daser *et al.*, 1994); 4–8 K*R*XIDKAA*K* tested peptide; lane 4, $X =$ Gly (*C. trachomatis GroEL* 117–125); lane 5, $X =$ Leu; lane 6, $X =$ Ana; lane 7, $X =$ Bna; lane 8, $X =$ Hpa. (*b*) Semi-quantitative measurement of the HLA-B*2705 heavy-chain bands, performed by densitometry, after loading with the studied peptide. The density of the heavy-chain band is a semi-quantitative indicator of the binding affinity of tested peptides for the HLA-B*2705 protein. The measured values are exactly correlated with the values of the binding affinity (Daser *et al.*, 1994).

as previously described (Daser *et al.*, 1994). The autoradiograph in Fig. 7(*a*) clearly show that all five peptides studied (lanes 4 to 8) could stabilize the HLA-B27 heavy chain but with different potencies. The density of the [^{35}S]methionine-labeled heavy-chain band (Fig. 7*b*) is dramatically enhanced in the presence of the three non-natural nonamers, when compared to the binding seen for both natural homologues. The density for the three non-natural nonapeptides is similar to that of the *GroEL* (284–292) control for which the half-maximum binding efficiency occurs at 0.5 μM (Daser *et al.*, 1994), while the density of the two natural homologues is comparable to that of the reference peptide with a half-maximum binding efficiency of 40 μM (Daser *et al.*, 1994). As predicted, the three non-natural nonapeptides are more potent ligands than the natural peptides with Gly or Leu at position *P*3. These predictions have recently been confirmed by binding studies on HLA-A*0201 peptides that ranked large hydrophobic amino acids (Trp, Tyr, Phe) at the first three positions that contribute the most to ameliorate the binding of nonapeptides to this allele (Parker, Bednarek & Coligan, 1994). In a recent study, Trp and Phe have been shown to be the amino acids that contributed the most to a tight binding to HLAB*2705, when only position 3 was modified (Fruci *et al.*, 1994). In our *in vitro* assembly assay, the three non-natural peptides were found to have a slightly better affinity for HLA-B*2705 than corresponding Phe and Trp homologues (unpublished data).

Concluding remarks

This study, using molecular modeling to explore novel ligands to a known structure, suggests that molecular-dynamics simulations of MHC–peptide bimolecular complexes are valuable tools for extending the existing MHC-binding motifs and for predicting potential T-cell epitopes as well as for the rational design of HLA inhibitors for the selective immunotherapy of autoimmune diseases to which class I HLA-B27 alleles are associated. Using rational structure-based drug design in combination with MD simulations, it was possible to predict successfully a significantly increased binding affinity of non-natural nonapeptides to the HLA-B*2705 protein. This prediction is fully supported by the semi-quantitative *in vitro* assembly assay where the ability of the five nonapeptides (*P*3 = Gly, Leu, Hpa, Bna, Ana) to stabilize the native conformation of the HLA-B*2705 heavy chain has been measured. The values of this assay are directly correlated to peptide titration data where the peptide concentration inducing 50% of the maximum binding is measured (Daser *et al.*, 1994), the results show clearly that the three non-natural ligands bind with higher affinity (0.5 μM) to the MHC protein than the two natural homologues (40 μM), just as the calculations predicted.

Current work is in progress to design non-peptidic inhibitors specific for HLA-B27 proteins and to investigate the CTL responses induced by the three non-natural nonamers and their immunogenicity.

The authors wish to thank the Schweizerischer Nationalfonds (Project No. 31-3597792) for sponsoring this work. The material and results of this work are partially described in the paper by Rognan *et al.* (Rognan, Scapozza, Folkers & Daser, 1995).

References

ADORINI, L., MULLER, S. CARDINAUX, F., LEHMANN, P. V., FALCIONI, F. & NAGY, Z. A. (1988). *Nature (London)*, **334**, 623–625.

BERENDSEN, H. J. C., POSTMA, J. P. M., VAN GUNSTEREN, W. F., DINOLA, A. & HAAK, J. R. (1984) *J. Chem. Phys.* **81**, 3684–3690.

BESLER, B. H., MERZ, K. M. & KOLLMAN, P. A. (1990). *J. Comput. Chem.* **11**, 431–439.

BJORKMAN, P. J. & PARHAM, P. (1990). *Annu. Rev. Biochem.* **59**, 253–288.

BJORKMAN, P. J., SAPER, M. A., SAMRAOUI, B., BENNETT, W. S., STROMINGER, J. L. & WILEY, D. C. (1987). *Nature (London)*, **329**, 506–512.

BREWERTON, D. A., CAFFREY, M., HART, F. D., JAMES, D. C. O., NICHOLLS, A. & STURROCK, R. D. (1973). *Lancet*, **1**, 904–907.

CONNOLLY, M. L. (1983). *J. Appl. Cryst.* **16**, 548–558.

DASER, A., HENNING, U. & HENKLEIN, P. (1994). *Mol. Immunol.* **31**, 331–336

DEWAR, M. J. S. & THIEL, W. (1977). *J. Am. Chem. Soc.* **99**, 4899–4907.

ELLIS, S. A., TAYLOR, C. & MCMICHAEL, A. J. (1982). *Human Immunol.* **5**, 49–59.

EVAVOLD, B. D., SLOAN-LANCASTER, J. & ALLEN, P. M. (1993). *Immunol. Today*, **14**, 602–609.

FALK, K., RÖTZSCHKE, O., STEVANOVIC, S., JUNG, G. & RAMMENSEE, H.-G. (1991). *Nature (London)*, **351**, 290–296.

FREMONT, D. H. MATSAMURA, M., STURA, E. A., PETERSON, P. A. & WILSON, I. A. (1992). *Science*, **257**, 919–927.

FRUCI, D., GRECO, G., VIGNETI, E., TANIGAKI, N., BUTLER, R. H. & TOSI, R. (1994). *Human Immunol.* **41**, 34–38.

GOODFORD, P. J. (1985). *J. Med. Chem.* **28**, 849–857.

GUO, H.-C., MADDEN, D. R., SILVER, M. L., JARDETZKY, T. S., STROMINGER, J. L. & WILEY, D. C. (1993). *Proc. Natl Acad. Sci. USA*, **90**, 8053–8057.

HUET, S., NIXON, D. F., ROTHBARD, J. B., TOWSEND, A., ELLIS, S. A. & MCMICHAEL, A. J. (1990). *Int. Immunol.* **2**, 311–316.

JORGENSEN, W. L., CHANDRASEKHAR, J., MADURA, J. D., IMPEY, R. W. & KLEIN, M. (1983). *J. Chem. Phys.* **70**, 926–935.

KINGSLEY, G. & SIEPER, J. (1993). *Immunol Today*, **14**, 387–391

KRUG, M. (1991). PhD thesis, Univ. of Tübingen, Germany.

MADDEN, D. R., GARBOCZI, D. N. & WILEY, D. C. (1993). *Cell*, **75**, 693–708.

MADDEN, D. R., GORGA, J. C., STROMINGER, J. L. & WILEY, D. C. (1991). *Nature (London)*, **353**, 321–325

MADDEN, D. R., GORGA, J. C., STROMINGER, J. L. & WILEY, D. C. (1992). *Cell*, **70**, 1035–1048.

MADDEN, D. R. & WILEY, D. C. (1992). *Curr. Opin. Struct. Biol.* **2**, 300–304.

PARKER, K. C., BEDNAREK, M. A. & COLIGAN, J. E. (1994). *J. Immunol.* **152**, 162–175.

PEARLMAN, D. A., CASE, D. A., CALDWELL, J. C., SEIBEL, G. L., SINGH, C., WEINER, P. & KOLLMAN, P. (1992). *AMBER* 4.0, Univ. of California, San Francisco, USA.

ROGNAN, D., SCAPOZZA, L., FOLKERS, G. & DASER, A. (1994). *Biochemistry*, **33**, 11476–11485.

ROGNAN, D., SCAPOZZA, L., FOLKERS, G. & DASER, A. (1995). *Proc. Natl Acad. Sci.* In the press.

ROGNAN, D., ZIMMERMANN, N., JUNG, G. & FOLKERS, G. (1992). *Eur. J. Biochem.* **208**, 101–113.

RÖTZSCKE, O., FALK, K., STEVANOVIC. S., GNAU, V., JUNG, G. & RAMMENSEE, H.-G. (1994). *Immunogenetics*, **39**, 74–77.

RYCKAERT, J. P., CICOTTI, G. & BERENDSEN, M. J. C. (1977). *J. Comput. Phys.* **23**, 327–341.

SAITO, Y., PETERSON, P. A. & MATSAMURA, M. (1993). *J. Biol. Chem.* **268**, 21309–21317.

SAPER, M. A., BJORKMAN, P. J. & WILEY, D. C. (1991). *J. Mol. Biol.* **219**, 277–319.

SILVER, M. L., GUO, H.-C., STROMINGER, J. L. & WILEY, D. C. (1992). *Nature (London)*, **360**, 367–369.

STEWART, J. J. P (1990). *J. Comput. Aided. Drug. Des.* **4**, 1–105.

TOWNSEND, A & BODMER, H. (1989). *Annu. Rev. Immunol.* **7**, 601–624.

TOWNSEND, A, ELLIOT, T., CERUNDOLO, V., FOSTER, L., BARBER, B. & TSE, A. (1990). *Cell*, **62**, 285–295.

Tripos Associates, Inc. (1992). *SYBYL Molecular Modeling System, Version* 5.40, Tripos Associates Inc., 1699 S. Hanley Road, Suite 303, St Louis, MO 63944, USA.

WEINER, S. J., KOLLMANN, P. A., CASE, D. A., SINGH, U. C., GHIO, C., ALAGONA, G., PROFETA, S. JR & WEINER, P. A. (1984). *J. Am. Chem. Soc.* **106**, 765–784.

ZHANG, W., YOUNG, A. C. M., IMARAI, M., NATHENSON, S. G. & SACHETTINI, J. C. (1992). *Proc. Natl Acad. Sci. USA*, **89**, 8403–8407.

ZINKERNAGEL, R. M. & DOHERTY, P. C. (1974). *Nature (London)*, **90**, 701–702.